

Supplementary Information for

Formation of stabilized vaterite nanoparticles via the introduction of uranyl into groundwater

Siyuan Wu^a, Jin Du^a, Jiebiao Li^{b*}, Mark Julian Henderson^a, Guangfeng Liu^c, Jianqiao Zhang^c, Na Li^c,

Alain Gibaud^d, Qiang Tian^{a*}

^aState Key Laboratory of Environment-friendly Energy Materials, School of Materials and Chemistry,

Southwest University of Science and Technology, Mianyang 621010, China

^bBeijing Research Institute of Uranium Geology, Beijing 100029, China

^cShanghai Advanced Research Institute, Chinese Academy of Sciences, Shanghai 201210, China

^dIMMM, Le Mans Université, Bld O. Messiaen, 72085 Le Mans, Cedex 9, France

Corresponding Authors:

*hgyljbiebiao@126.com (J Li); tianqiang@swust.edu.cn (Q. Tian)

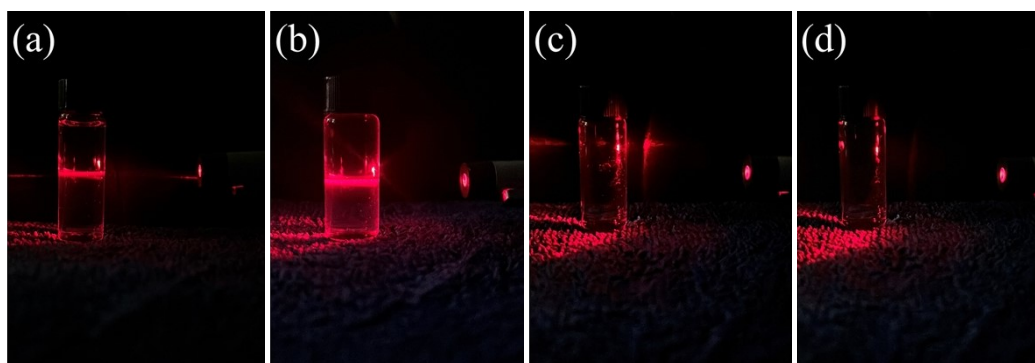


Fig. S1 Tyndall phenomena of the mixture of the Beishan groundwater and uranyl nitrate: (a) freshly prepared; (b) stored for one year at room temperature. The controlled sample of groundwater (c) and uranyl nitrate solution (d) under red laser.

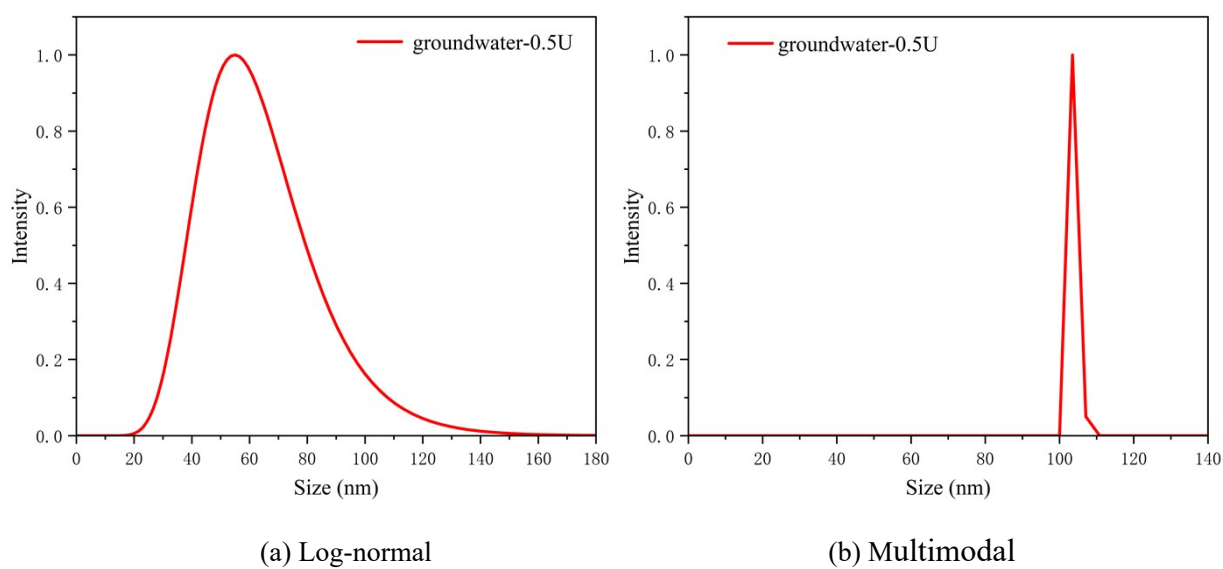


Fig. S2. The intensity-weighted log-normal (a) and multimodal (b) size distributions of hydrodynamic size.

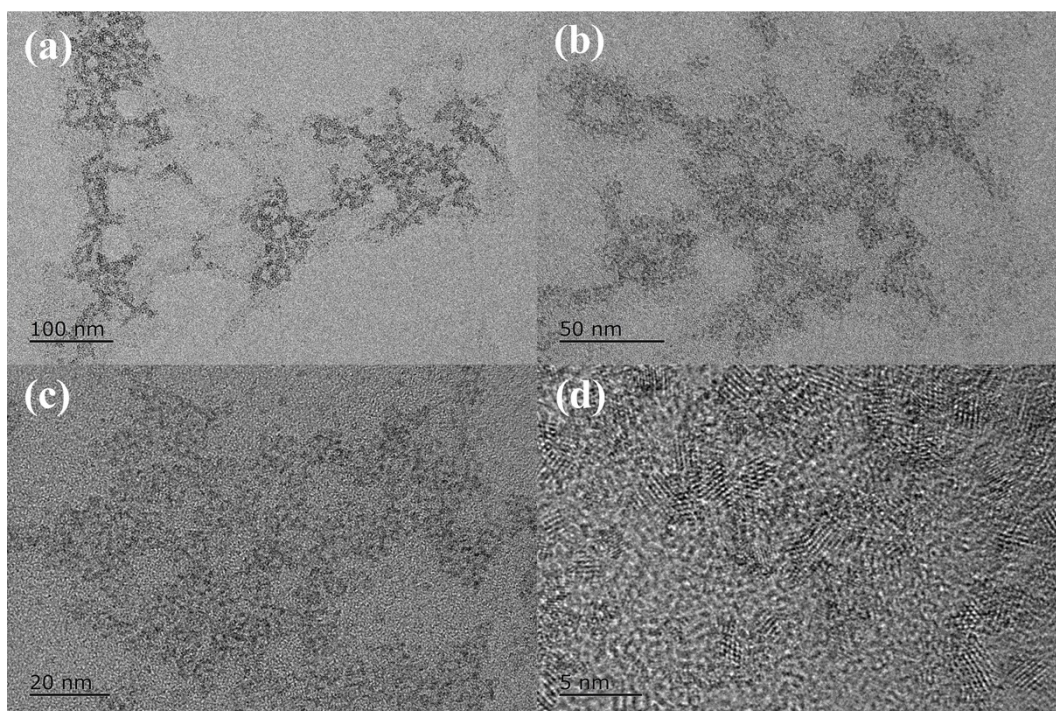


Fig. S3 TEM images obtained from the groundwater-0.5 U

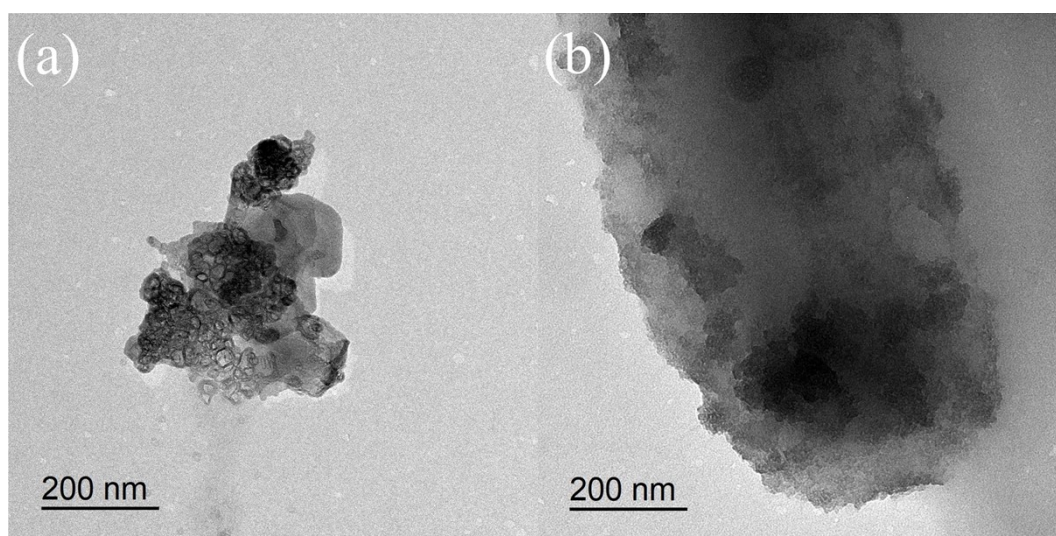


Fig. S4 TEM images obtained from the pure Beishan groundwater.

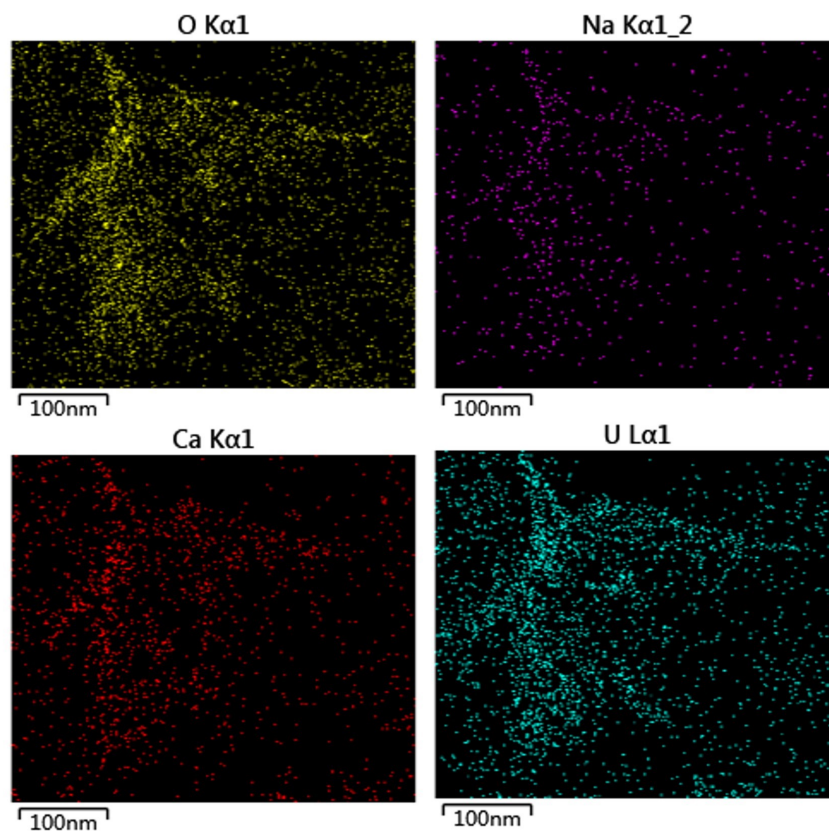
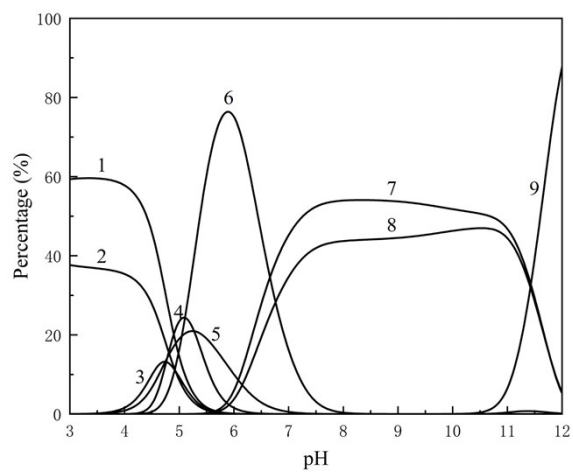


Fig. S5 TEM element mapping images of O, Na, Ca, and U obtained from groundwater-3U.



1— $\text{UO}_2\text{SO}_4(\text{aq})$; 2— UO_2^{2+} ; 3— $(\text{UO}_2)_2(\text{OH})_2^{2+}$; 4— $(\text{UO}_2)_3(\text{OH})_5^+$; 5— $\text{UO}_2\text{CO}_3(\text{aq})$;
 6— $(\text{UO}_2)_2\text{CO}_3(\text{OH})_3^-$; 7— $\text{Ca}_2\text{UO}_2(\text{CO}_3)_3(\text{aq})$; 8— $\text{CaUO}_2(\text{CO}_3)_3^{2-}$; 9— $\text{UO}_2(\text{OH})_3^-$

Fig. S6 Influence of pH on the distribution of uranium species (>5%) in groundwater-0.5 U ([U] = 0.5 mmol/L, T = 25 °C).

Table S1 Thermodynamic data of uranium at 25 °C.

Chemical reactions	log K
$\text{UO}_2^{2+} + \text{H}_2\text{O} = \text{UO}_2\text{OH}^+ + \text{H}^+$	-5.25
$\text{UO}_2^{2+} + 3\text{H}_2\text{O} = \text{UO}_2(\text{OH})_3^- + 3\text{H}^+$	-20.25
$\text{UO}_2^{2+} + 2\text{OH}^- = \text{UO}_2(\text{OH})_2$	-10.31
$2\text{UO}_2^{2+} + \text{H}_2\text{O} = (\text{UO}_2)_2\text{OH}^{3+} + \text{H}^+$	-2.70
$2\text{UO}_2^{2+} + 2\text{H}_2\text{O} = (\text{UO}_2)_2(\text{OH})_2^{2+} + 2\text{H}^+$	-5.62
$3\text{UO}_2^{2+} + 4\text{H}_2\text{O} = (\text{UO}_2)_3(\text{OH})_4^{2+} + 4\text{H}^+$	-11.90
$3\text{UO}_2^{2+} + 5\text{H}_2\text{O} = (\text{UO}_2)_3(\text{OH})_5^+ + 5\text{H}^+$	-15.55
$3\text{UO}_2^{2+} + 7\text{H}_2\text{O} = (\text{UO}_2)_3(\text{OH})_7^- + 7\text{H}^+$	-32.20
$4\text{UO}_2^{2+} + 7\text{H}_2\text{O} = (\text{UO}_2)_4(\text{OH})_7^+ + 7\text{H}^+$	-21.90
$\text{UO}_2^{2+} + \text{SO}_4^{2-} = \text{UO}_2\text{SO}_4$	3.15
$\text{UO}_2^{2+} + 2\text{SO}_4^{2-} = \text{UO}_2(\text{SO}_4)_2^{2-}$	4.14
$\text{UO}_2^{2+} + \text{Cl}^- = \text{UO}_2\text{Cl}^+$	0.17
$\text{UO}_2^{2+} + \text{Cl}^- = \text{UO}_2\text{Cl}_2$	-1.10
$\text{UO}_2^{2+} + \text{CO}_3^{2-} = \text{UO}_2\text{CO}_3$	9.94
$\text{UO}_2^{2+} + 2\text{CO}_3^{2-} = \text{UO}_2(\text{CO}_3)_2^{2-}$	16.61
$\text{UO}_2^{2+} + 3\text{CO}_3^{2-} = \text{UO}_2(\text{CO}_3)_3^{4-}$	21.84
$2\text{UO}_2^{2+} + 3\text{H}_2\text{O} + \text{CO}_3^{2-} = (\text{UO}_2)_2\text{CO}_3(\text{OH})_3^- + 3\text{H}^+$	-0.86
$\text{Ca}^{2+} + \text{UO}_2(\text{CO}_3)_3^{4-} = \text{CaUO}_2(\text{CO}_3)_3^{2-}$	5.33*
$2\text{Ca}^{2+} + \text{UO}_2(\text{CO}_3)_3^{4-} = \text{Ca}_2\text{UO}_2(\text{CO}_3)_3$	8.70*
$\text{Mg}^{2+} + \text{UO}_2(\text{CO}_3)_3^{4-} = \text{MgUO}_2(\text{CO}_3)_3^{2-}$	2.61*

*Jo Y, Kirishima A, Kimuro S, et al. Formation of $\text{CaUO}_2(\text{CO}_3)_3^{2-}$ and $\text{Ca}_2\text{UO}_2(\text{CO}_3)_3(\text{aq})$ complexes at variable temperatures (10 – 70 °C). Dalton Transactions, 2019, 48(20): 6942–6950.

* Jo Y, Kim H K, Yun J I. Complexation of $\text{UO}_2(\text{CO}_3)_3^{4-}$ with Mg^{2+} at varying temperatures and its effect on U(VI) speciation in groundwater and seawater. Dalton Transactions, 2019, 48(39): 14769–14776.

Table S2 *d*-spacings derived from the SAED and HRTEM image of groundwater-3U.

JCPDS 87-1714 Clarkeite $[\text{Na}(\text{UO}_2)\text{O}(\text{OH})]$		SAED	HRTEM
hkl	<i>d</i> (Å)	<i>d</i> (Å)	<i>d</i> (Å)
003	5.89		5.86
012	3.19	3.20	
104	2.71	2.71	
113	1.87	1.92	
116	1.64	1.61	

Table S3 The possible precipitated minerals with SI > 0 from the Beishan groundwater simulated by PHREEQC ([U] = 0.5 mmol/L, T = 25 °C, pH = 7.0).

Phase	Chemical formula	Log K	Log IAP	SI
Andersonite	$\text{Na}_2\text{CaUO}_2(\text{CO}_3)_3 \cdot 6\text{H}_2\text{O}$	-37.50	-34.47	3.03
Bayelite	$\text{Mg}_2\text{UO}_2(\text{CO}_3)_3 \cdot 18\text{H}_2\text{O}$	-36.60	-34.93	1.67
Becquerelite	$\text{Ca}(\text{UO}_2)_6\text{O}_4(\text{OH})_6 \cdot 8\text{H}_2\text{O}$	40.5	40.88	0.38
Clarkeite	$\text{Na}(\text{UO}_2)\text{O}(\text{OH})$	9.02	10.23	1.21
Calcite	CaCO_3	1.85	1.97	0.13
Liebigite	$\text{Ca}_2\text{UO}_2(\text{CO}_3)_3 \cdot 10\text{H}_2\text{O}$	-37.90	-33.92	3.98
Magnesite	MgCO_3	-8.91	-8.80	0.11